Photosynthetic oxygenation for urine nitrification

1 Photosynthetic oxygenation for urine nitrification

2 Short title: Photosynthetic oxygenation for urine nitrification

3

4 **Maarten Muys[1], Joeri Coppens[2], Nico Boon[2] , Siegfried E. Vlaeminck[1, 2, *]**

5

6 [1] Research Group of Sustainable Energy, Air and Water Technology, Department of
7 Bioscience Engineering, University of Antwerp, Groenenborgerlaan 171, 2020 Antwerpen,
8 Belgium.

9 [2] Center for Microbial Ecology and Technology (CMET), Ghent University, Coupure Links
10 653, 9000 Gent, Belgium.

11 [*] Corresponding author: Siegfried.Vlaeminck@UAntwerpen.be

Abstract

Human urine accounts for only a fraction of the sewage volume, but it contains the majority of valuable nutrient load in wastewater. In this study, synthetic urine was nitrified in a closed photo-bioreactor through photosynthetic oxygenation by means of a consortium of microalgae and nitrifying bacteria. In-situ production of oxygen by photosynthetic organisms has the potential to reduce the energy costs linked to conventional aeration. This energy efficient strategy results in stable urine for further nutrient recovery, while part of the nutrients are biologically recovered in the form of valuable biomass. In this study, urine was nitrified for the first time without conventional aeration at a maximum photosynthetic oxygenation rate of 160 mg O_2 $gVSS^{-1}$ d^{-1}. A maximum volumetric nitrification rate of 67 mg N L^{-1} d^{-1} was achieved on 12% diluted synthetic urine. COD removal efficiencies were situated between 44 and 83% at a removal rate of 24 mg COD $gVSS^{-1}$ d^{-1}. After 180 days, microscopic observations revealed that *Scenedesmus* sp. was the dominant microalga. Overall, photosynthetic oxygenation for urine nitrification is promising as highly electricity efficient approach for further nutrient recovery.

Keywords

Activated sludge, High rate algal ponds, Microalgal-bacterial consortium, Photo-aeration, Resource recovery, Source separation

Introduction

In the context of sustainable resource management, the transition towards energy-efficient and resource-recovery focused wastewater treatment is pivotal. For nutrients such as nitrogen (N) and phosphorus (P), the diluted characteristics of domestic wastewater make direct nutrient recovery technologically challenging and resource intensive. Nutrient recovery is therefore recommended for more concentrated waste streams, such as manure, digestate or urine (Verstraete *et al.* 2016). Urine accounts for only 1% of the total domestic wastewater volume, while it contains approximately 40% of the phosphorus load, 69% of the nitrogen load, and 60% of the potassium load arriving at municipal wastewater treatment plants (Kujawa-Roeleveld & Zeeman 2006). This makes it a valuable target stream for nutrient recovery.

While direct application of urine as fertilizer has been common practice in many rural societies around the world, the high water content makes transportation and application costly, while the high urine salinity causes soil salinization (Basakcilardan-Kabakci *et al.* 2007). In addition, potential presence of pathogens and pharmaceuticals further increases health concerns towards farmers and consumers (Udert *et al.* 2006). More advanced chemical and biological nutrient recovery strategies have therefore been demonstrated, such as ammonia stripping, struvite precipitation and microalgae cultivation (Maurer *et al.* 2006; Tuantet *et al.* 2013). Urine is, however, highly unstable, as urea hydrolysis through bacterial urease results in the production of ammonia and bicarbonate. The subsequent pH rise induces nutrient losses through unwanted phosphate precipitation and ammonia volatilization and concomitant odour and toxicity issues (Udert *et al.* 2003).

Chemical stabilization, for example through acid dosage, or biological stabilization through nitrification, have therefore been suggested as a pre-treatment step prior to nutrient recovery (Maurer *et al.* 2006; Feng *et al.* 2008). Biological urine stabilization through nitrification converts volatile ammonia to nitrate, thereby allowing for long-term storage and further use as

55 agricultural fertilizer or for microalgae cultivation. However, oxygen requirements associated
56 to the nitrification process result in large energy demands due to energy-intensive
57 conventional aeration. Based on an oxygenation efficiency of 1 kg O_2 kWh^{-1} (Metcalf &
58 Eddy 2002) and a urine COD/N ratio of 0.8, the electricity need for nitrification and COD
59 oxidation with conventional aeration is 31 kWh m^{-3} urine (SRT: 6.66 days; 25°C).

60 An alternative for conventional aeration is photosynthetic oxygenation, or in-situ oxygen
61 production by photosynthetic organisms such as microalgae. By providing the oxygen
62 demand for autotrophic nitrification and heterotrophic carbon oxidation through in-situ
63 photosynthesis while consuming heterotrophically produced carbon dioxide, electricity costs
64 and greenhouse gas emissions affiliated to conventional aeration and wastewater treatment
65 can be reduced (Praveen & Loh 2015). In addition, the produced microalgal-bacterial biomass
66 can be used for energy production (anaerobic digestion), as a resource for the production of
67 high-value biochemical and biofuels or it can be applied as slow-release fertilizer or microbial
68 protein (Tuantet *et al.* 2013; Coppens *et al.* 2016).

69 The combination of photosynthetic oxygenation with nitrification or nitrification-
70 denitrification has been described in both high-rate algal ponds (HRAP) and in photo-
71 bioreactors, for various waste-streams (Table 1). Karya *et al.* (2013) achieved a volumetric
72 nitrification rate of 43 mg N L^{-1} d^{-1} and photo-oxygenation rate of 140 mg O_2 $gVSS^{-1}$ d^{-1},
73 while van der Steen *et al.* (2015) reported a volumetric nitrification rate of 46 mg N L^{-1} d^{-1}
74 and photo-oxygenation rate of 234 mg O_2 $gVSS^{-1}$ d^{-1}. Furthermore, direct microalgae
75 cultivation on urine has been established (Adamsson 2000; Yang *et al.* 2008; Tuantet *et al.*
76 2013) and superior microalgal growth on nitrified urine compared to untreated urine has been
77 demonstrated (Coppens *et al.* 2016).

78 Table 1. Application of photosynthetic oxygenation by means of algal-bacterial consortia for
79 the treatment of various liquid waste-streams (HRAP: high-rate algal pond; PBR: photo-

bioreactor; SBR: sequencing batch reactor; SRT: solids retention time; HRT: hydraulic retention time; CSTR: continuously stirred tank reactor).

Waste stream	Consortium	Set-up and operation	N-loading rate (mg N L^{-1} d^{-1})	Volumetric nitrification rate (mg N L^{-1} d^{-1})	Biomass specific nitrification rate (mg N $gVSS^{-1}$ d^{-1})	Nitrification efficiency (%)	COD oxidation rate (mg COD $gVSS^{-1}$ d^{-1})	Photo-oxygenation rate (mg O_2 $gVSS^{-1}$ d^{-1})	Reference
10% swine manure	Inoculum from stabilization pond treating domestic wastewater	Outdoor HRAP; HRT: 10 d	30	9	10	30	73	110	de Godos *et al.* (2009)
Modified BG-11 medium	*S. quadricauda*, nitrifiers	PBR as SBR; SRT: 15 - 30 d; 60 µmol m^{-2} s^{-1}	50	43	31	85	0	140	Karya *et al.* (2013)
Pre-treated sewage	*C. vulgaris*, activated sludge	Continuous PBR; SRT: 15 d; HRT: 1.5 d; 2000 µmol m^{-2} s^{-1}	50	2	0.97	2.9	184	154	Gutzeit *et al.* (2005)
10% (v/v) molasses wastewater	Municipal activated sludge	PBR as SBR; HRT: 5 d; 17W LED	43	36	28	83	47	168	Tsioptsias *et al.* (2017)
Modified BG-11 medium	Microalgae, activated sludge	PBR as CSTR; HRT: 1 d; SRT: 15 d; 66 µmol m^{-2} s^{-1}	66	46	48	70	0	234	van der Steen *et al.* (2015)
12% synthetic urine	**Microalgae, activated sludge**	**Semi-continuous PBR; HRT: 6.67 d; SRT = HRT; 300 µmol m^{-2} s^{-1}**	**97**	**67**	**31**	**64**	**24**	**160**	**This study**

Photosynthetic oxygenation for urine nitrification has so far not been documented. The goal of this study was to develop a micoalgal-bacterial consortium for urine nitrification through photosynthetic oxygenation. The influence of salinity and ammonium concentration on microalgal growth was determined and subsequently, a photo-bioreactor was operated for urine nitrification in the absence of external aeration.

Methods

Nitrifying sludge and microalgae

The inoculum comprised of commercially available nitrifying activated sludge (Avecom, Belgium), the microalgal species *Chlorella* sp., *Haematococcus* sp., *Desmodesmus* sp., *Ankistrodesmus* sp., *Pediastrum duplex*, *Chlorella vulgaris* and *Nannochloropsis* sp. (MARBIO, UGent) and microalgae acquired from a grassland pond (Ghent, Belgium). The initial biomass concentration was set at 0.7 g VSS L^{-1} of which half was microalgal biomass, the other half activated sludge. Prior to inoculation, all microalgae were cultivated at 25 ± 1 °C in Enriched Seawater Artificial Water (ESAW) medium made with artificial seawater

96 (Harrison *et al.* 1980), because of its salt concentration in the range of that of urine. The
97 cultures were aerated with sterile air and continuously illuminated (Philips TL-D 90 De Lux
98 36W).

99 *Influence of ammonium and salt concentration on microalgal growth*
100 A mixture of all microalgae was exposed to ESAW medium containing 1, 2, 3.5 and 5 g L^{-1}
101 NaCl and 50, 100, 200 and 1000 mg NH_4^+-N L^{-1}, brought at pH 6 with a phosphate buffer.
102 The experiment was realized in quadruplicate in 96 well micro titer plates (300µL per well).
103 The optical density (OD) was measured daily at 620 nm with a plate reader (Tecan Infinite),
104 after shaking. Each well was inoculated between 0.10 and 0.17 (OD620). The plates were
105 incubated in an orbital shaking incubator at 25°C for 160 hours.

106 *Photo-bioreactor design and operation*
107 A Plexiglas, gastight, bubble column photo-bioreactor with a working volume of 4 Litre (ø 12
108 cm; height 50 cm), was operated in semi-continuous mode (Figure 1). The illuminated surface
109 area was 0.16 m² resulting in a volume to surface ratio of 0.025 m^3 m^{-2}. Three fluorescent
110 growth lamps (Grolux T5, 24W, Sylvania) provided a photon flux density of 300 µmol PAR
111 m^{-2} s^{-1}, measured in a straight angle from the lamp at the outer reactor wall (Fieldscout
112 quantum light meter, USA). Liquid recirculation at 0.5 L min^{-1} and headspace gas
113 recirculation at 6 L min^{-1} took place. CO_2 and N_2 gas were dosed in a 10/90 (v/v) ratio
114 (Bronkhorst high-tech EL-FLOW select mass flow meter/controller) as 1% of the gas
115 recirculation flow. Where mentioned, co-aeration with compressed air was applied at 0.25 L
116 O_2 L $reactor^{-1}$ h^{-1}. The pH was controlled between 6.5 and 7 (Prominent dulcometer; pH
117 electrode dulcotest PHEP-112). The temperature was kept at 25 ± 1 °C by operating in a
118 temperature controlled room.

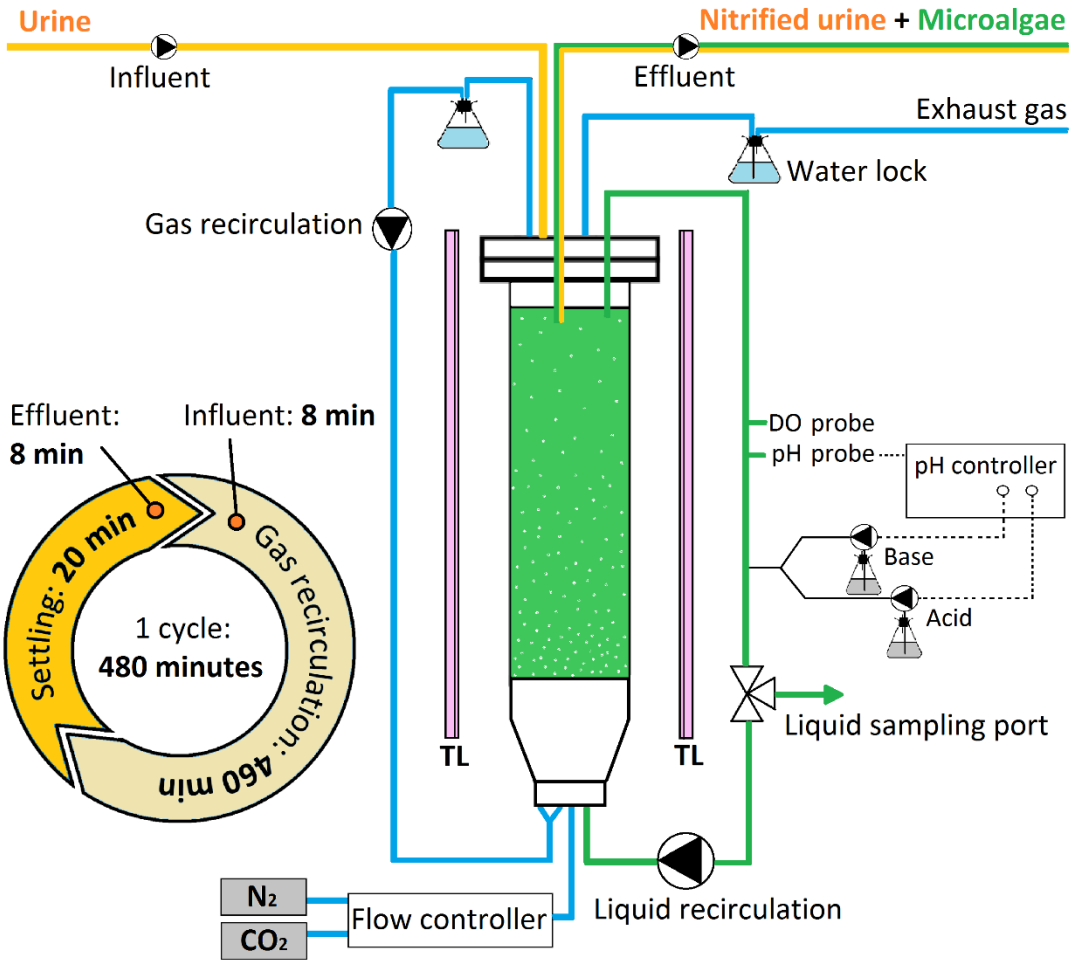

Figure 1. Schematic overview of the photo-bioreactor bubble column and the timeline for one operation cycle of 8 hours. Full lines: liquid; Dotted lines: electric signal; Blue = gas flow; Green = bioreactor content.

Initially, 10% diluted synthetic urine medium (Brooks & Keevil 1997) with additional trace element solutions (Kuai & Verstraete 1998) was fed, implying a nitrogen loading rate of 50 mg N L^{-1} d^{-1}. The influent electrical conductivity was altered to that of a 33% dilution of urine (6.66 mS cm^{-1}) using NaCl. The nitrogen loading was distributed over time using three cycles of 8 hours per day. Influent was dosed during the first 8 minutes of each cycle during gas recirculation, while effluent was extracted during the last 8 minutes of each cycle at the end of the settling phase.

A nitrogen conversion balance was made to calculated how much of the incoming nitrogen was nitrified and how much was assimilated by the microalgae, nitrifiers and heterotrophs. This was done over 6 periods (I to VI) of each 7 days, just before an operational change took

133 place **(Table S1)**. Incoming nitrogen was defined as nitrogen available for nitrification and for
134 biomass growth, meaning the average total influent nitrogen together with the average
135 Kjeldahl and nitrite nitrogen present in the reactor. Since ammonium is the preferred
136 microalgal nitrogen source, it was assumed that nitrate was not assimilated. Incoming
137 nitrogen can accumulate in the reactor unconverted or in the form of biomass, or it can be
138 removed with the effluent as such or in the form of biomass. The amount of biomass
139 assimilated nitrogen removed with the effluent was calculated based on the mean biomass
140 concentration in the reactor and the assumption that effluent equalled reactor biomass
141 concentration. The biomass nitrogen content was determined by analysing filtered (0.45 μm)
142 versus non-filtered reactor content for Kjeldahl-N. Nitrogen assimilation in nitrifying biomass
143 was calculated based on the stoichiometry of nitrification (equation 1; Metcalf & Eddy
144 (2002)) and effluent nitrate concentrations.

145 $NH_4^+ + 1.863O_2 + 0.098CO_2 \rightarrow 0.0196C_5H_7NO_2 + 0.98NO_3^- + 0.0941H_2O + 1.98H^+$ (1)

146 Nitrogen assimilation by heterotrophic bacteria was calculated based on COD removal and
147 observed heterotrophic biomass yield (Metcalf & Eddy 2002). By subtracting the nitrogen
148 assimilated in nitrifier and heterotrophic biomass from the total effluent biomass nitrogen,
149 microalgal nitrogen assimilation was calculated.

150 *Sampling and analytical methods*

151 Every 2 days, samples of influent and bulk reactor solution at the end of a cycle were filtered
152 (0.45 μm Chromafil Xtra, Machery-Nagle, PA, USA) and stored at 4°C. The concentration of
153 ammonium was determined following the standard method of Nessler (Greenberg *et al.* 1992)
154 or according to standard methods (APHA, 1992). Kjeldahl nitrogen was also analysed
155 according to the standard methods (APHA, 1992). Organic nitrogen was determined as the
156 difference between Kjeldahl nitrogen and ammonium nitrogen. Nitrite and nitrate were

analysed with ion chromatography (IC 761, Compact, Methrom AG, Swiss). COD was determined photometrical (Nanocolor COD 160; Machery-Nagel, PA, USA). Total Suspended Solids (TSS) and Volatile Suspended Solids (VSS) were measured according the standard methods (APHA, 1997). The dissolved oxygen (DO) concentration was measured daily (Hach HQ40d) and electrical conductivity (EC) weekly (Consort C833). Reactor biomass was analysed with light microscopy (Zeiss Axioskop 2 plus). During photo-bioreactor operation, AOB and NOB nitrification activities were determined regularly following a standardized protocol (Coppens *et al.* 2016).

Results and discussion

Influence of ammonium and salt concentration on algal growth

Since fresh unhydrolysed urine contains a high salinity (± 20 mS cm^{-1}) and urea nitrogen concentration (5 g N L^{-1} for synthetic urine), the influence of different salt and ammonium concentrations was investigated on the growth of a mixture of all microalgal species. Four different salinities (1, 2, 3.5 and 5 g L^{-1} NaCl, corresponding to 4.54, 6.55, 9.95 and 13.60 mS cm^{-1}, respectively) and ammonium concentrations (50, 100, 250 and 1000 mg NH_4^+-N L^{-1}), were applied (Figure 2). A longer lag phase was observed at salt concentrations equal to or higher than 3.5 g NaCl L^{-1}. This might be due to the predominance of fresh water microalgal species. Results indicate that a concentration of 50 mg NH_4^+-N L^{-1} is preferred. Since no significant change in growth was observed for the mixed culture up to 2 g L^{-1} NaCl, corresponding to a salinity of 6.55 mS cm^{-1}, these tests indicate that the salinity of roughly 2 mS cm^{-1} for a 10% dilution of synthetic urine, will not inhibit microalgal growth. In contrast, ammonium concentrations (500 mg NH_4^+-N L^{-1} for a 10% diluted urine solution) could result in slower microalgal growth if ammonium accumulates in the PBR, depending on the nitrogen loading rate and nitrification activity.

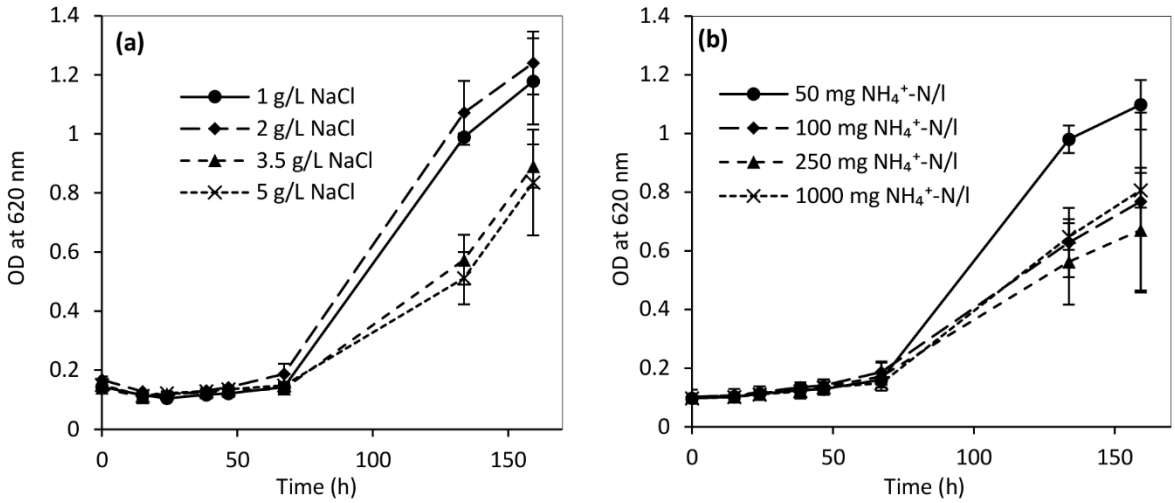

Figure 2. Growth of a mixture of all microalgal species exposed to (a) different salinities (1, 2, 3.5 and 5 g L^{-1}) and (b) ammonium concentrations (50, 100, 250 and 1000 mg NH_4^+-N L^{-1}) at 1 g L^{-1} NaCl.

Nitrogen evolution in the PBR

Start-up phase

During the first 15 days of reactor operation, nitrogen removal efficiencies between 60 and 95% (Figure 3 (a)) were achieved, but no nitrate accumulation was observed. COD removal efficiencies fluctuated between 61 and 93% (Figure 3 (d)) with a maximum COD removal rate of 45 mg COD $gVSS^{-1}$ d^{-1} at day 15. The DO concentration fluctuated around 3.6 ± 2.6 mg L^{-1}, indicating sufficient photo-oxygenation. An estimated 22% of the incoming nitrogen was assimilated, 51% accumulated in the reactor or was unconverted and removed with the effluent (Figure 4). The remaining 27% of incoming nitrogen was assumed to be lost due to ammonia stripping and denitrification.

To stimulate nitrification, at day 15, the reactor was re-inoculated with 1 g VSS L^{-1} of commercially available nitrifying inoculum (Avecom, Belgium). The high calcium carbonate content of the inoculum resulted in a decrease in VSS/TSS ratio from 0.83 to 0.42. Although, DO concentrations between 0.6 and 2 mg L^{-1} indicated successful photo-oxygenation, re-inoculation did not result in nitrification. However, activity tests demonstrated the low nitrification potential of the PBR biomass in both, fresh medium and reactor supernatant.

201 Additionally, no inhibitory effect was observed of reactor supernatant on new nitrifying
202 inoculum (Figure 5 (a)).

203 To increase oxygen concentrations and stimulate nitrification, co-aeration with compressed
204 air was started at day 25 at a flow rate of 0.25 L O_2 $L_{reactor}^{-1}$ h^{-1}. Complete nitrogen removal
205 was obtained (Figure 3 (a)) and nitrogen assimilation (77%) in microbial biomass remained
206 the dominant nitrogen removal pathway, with 76% assimilated as microalgal and 1% as
207 chemoheterotrophic biomass (Figure 4).

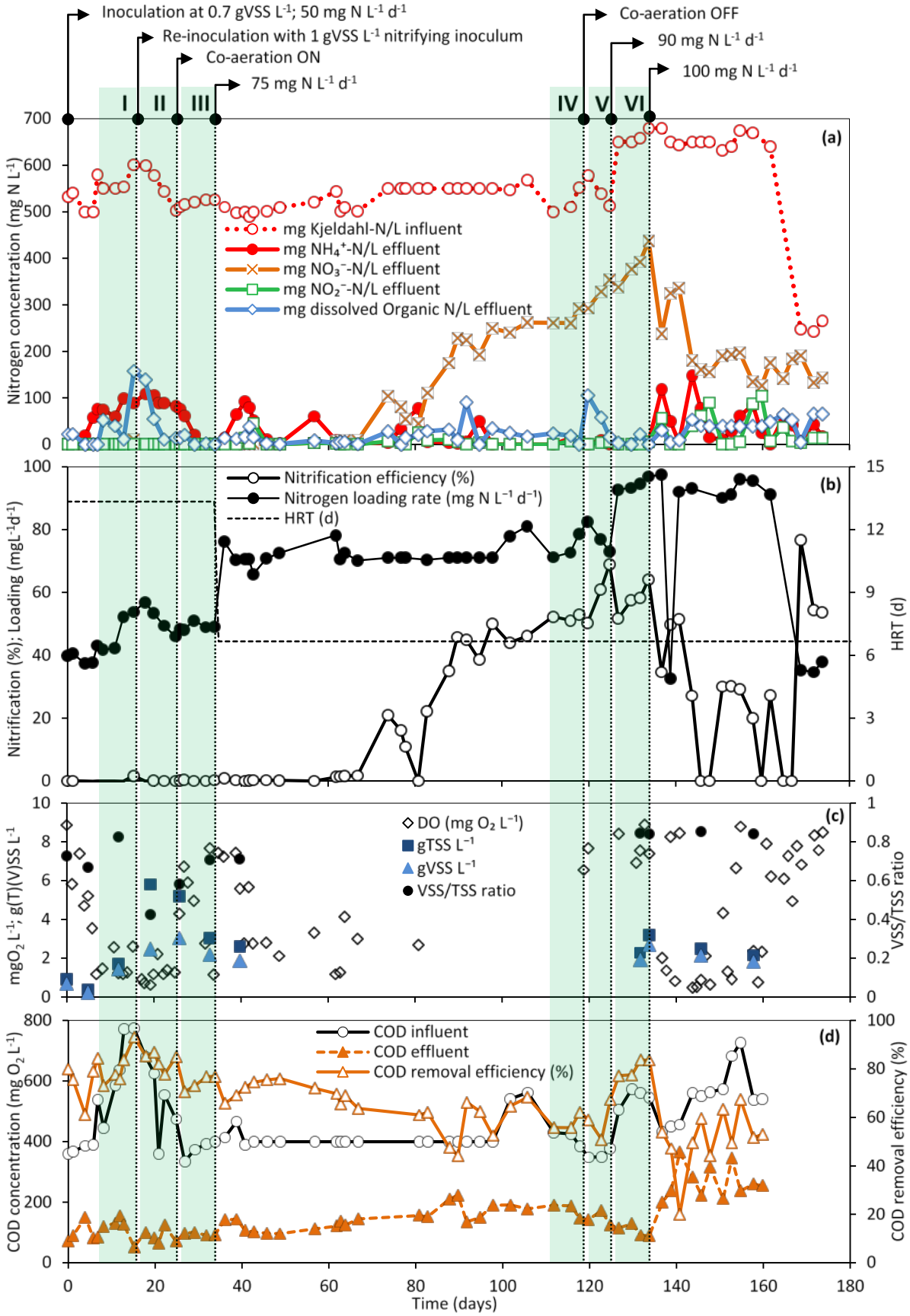
Inoculation at 0.7 gVSS L-1; 50 mg N L-1 d-1
Re-inoculation with 1 gVSS L-1 nitrifying inoculum
Co-aeration ON
75 mg N L-1 d-1
Co-aeration OFF
90 mg N L-1 d-1
100 mg N L-1 d-1
I
II
III
IV
V
VI
(a)
Nitrogen concentration (mg N L-1)
mg Kjeldahl-N/L influent
mg NH4+-N/L effluent
mg NO3--N/L effluent
mg NO2--N/L effluent
mg dissolved Organic N/L effluent
(b)
Nitrification (%); Loading (mgL-1d-1)
HRT (d)
Nitrification efficiency (%)
Nitrogen loading rate (mg N L-1 d-1)
HRT (d)
(c)
mgO2 L-1; g(T)(V)SS L-1
VSS/TSS ratio
DO (mg O2 L-1)
gTSS L-1
gVSS L-1
VSS/TSS ratio
(d)
COD concentration (mg O2 L-1)
COD removal efficiency (%)
COD influent
COD effluent
COD removal efficiency (%)
Time (days)

208

209

Figure 3. (a) PBR influent and effluent nitrogen species (mg N L^{-1}); (b) Nitrogen loading rate (g N L^{-1} d^{-1}), nitrification efficiency (%) and hydraulic retention time (HRT) (d); (c) DO, TSS and VSS concentration; (d) Influent and effluent COD concentrations and COD removal efficiency, during 174 days of PBR operation. Changes in reactor operation are indicated with arrows while the zones from I to VI indicate the periods just before a change in reactor operation, over which a 7 day nitrogen conversion balance was made.

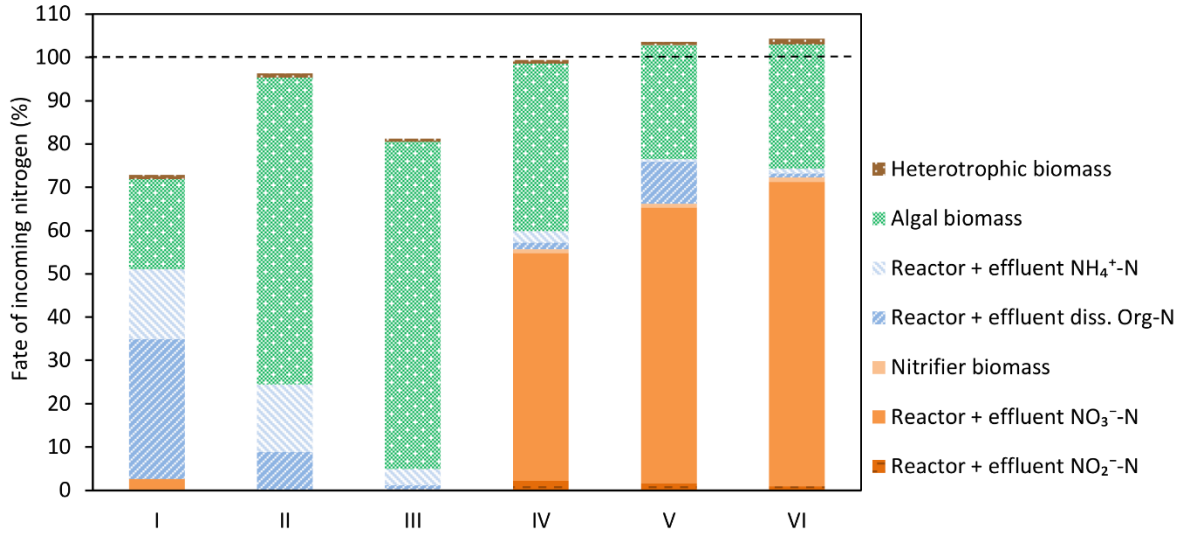

Figure 4. Nitrogen (N) conversion balance over the periods I to VI. Incoming N is defined as the average total influent N together with the average Kjeldahl and nitrite-Npresent in the reactor. Incoming N can accumulate in the PBR or can be removed with the effluent.

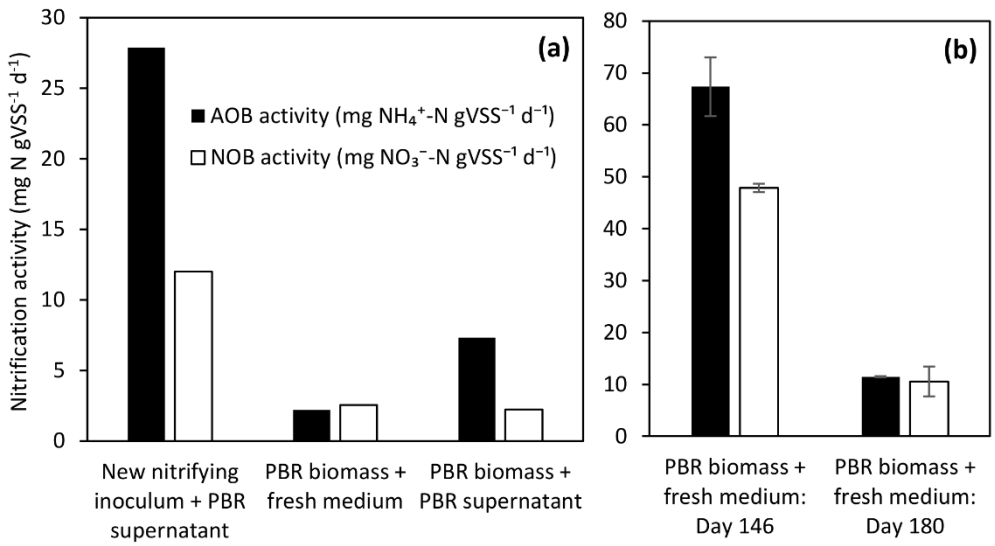

Figure 5. Nitrification activity for AOB and NOB.(a) Day 19. New nitrifying inoculum exposed to PBR supernatant; PBR biomass exposed to PBR supernatant; PBR biomass exposed to fresh medium.(b) Day 146 and 180.PBR biomass exposed to fresh medium.

Nitrification phase

From day 55 onwards, accumulation of nitrate indicated successful nitrification, while the COD removal efficiency was situated between 44 and 83%. Starting from day 110,

nitrification efficiencies higher than 50% were obtained. Therefore, at day 118, external aeration was stopped and since oxygen levels remained above 6 mg O_2 L^{-1}, photosynthetic oxygenation was sufficient to sustain nitrification and organic carbon oxidation. At day 134, nitrification efficiency reached 64% at a nitrogen loading rate of 97 mg N L^{-1} d^{-1} (12% synthetic urine) (Figure 3 (b)). Furthermore, well-settling microbial biomass was obtained, as indicated by the low sludge volume index (SVI_{30}) of 58.06 ml g^{-1}.

The increase of nitrogen loading rate to 100 mg N L^{-1} d^{-1} (15% dilution of synthetic urine) at day 134 resulted in a nitrification efficiency decline to values lower than 30% and reduction in biomass concentration to 2.14 gVSS L^{-1} at day 145. Nitrification batch activity tests demonstrated maximum volumetric ammonium and nitrite oxidation rates of 122 mg N L^{-1} d^{-1} and 87 mg N L^{-1} d^{-1}, which is higher than the nitrogen loading rates (Figure 5 (b)). A dissolved oxygen concentration below 1 mg L^{-1} indicated a drop in photo-aeration rate.

Between day 146 and 167, nitrification efficiency fluctuated between 0 and 30% and at day 168, the nitrogen loading rate was decreased to 35 mg N L^{-1} d^{-1}. From day 168 until 180, nitrification efficiencies remained between 52% and 53%. At day 180, a last activity test was performed (Figure 5 (b)), demonstrating that both AOB and NOB activity decreased to 12 mg NH_4-N $gVSS^{-1}$ d^{-1} and 11 mg NH_4-N $gVSS^{-1}$ d^{-1}, respectively.

PBR nitrification efficiency and photosynthetic oxygenation

The maximum achieved volumetric nitrification rate was 67 mg N L^{-1} d^{-1} at a loading rate of 97 mg N L^{-1} d^{-1}, which is higher than in the outdoor HRAP described by de Godos *et al.* (2009), where a volumetric nitrification rate of 9 mg N L^{-1} d^{-1} was achieved at a loading rate of 30 mg N L^{-1} d^{-1}. Karya *et al.* (2013) nitrified artificial wastewater supported by photo-oxygenation in an algal-bacterial consortium at a nitrogen loading rate of 50 mg N L^{-1} d^{-1} and maximum volumetric nitrification efficiency of 43 mg N L^{-1} d^{-1}. This artificial wastewater

did, however, not contain COD and all nitrogen was present as ammonium. van der Steen *et al.* (2015) reached a comparable volumetric nitrification rate of modified BG-11 medium of 46 mg N L^{-1} d^{-1} (Table 1).

The observed sudden nitrification activity in this study, could be the consequence of adaptation of the nitrifying community to light, since it is known that AOB and NOB are inhibited by light (Vergara *et al.* 2016). Guerrero and Jones (1996) studied light inhibition on marine AOB and NOB and concluded that photo-inhibition is species-specific and dependent on light intensity, lighting period and wavelength. AOB were found to be more sensitive to blue light than NOB, while cool-white fluorescent light inhibited AOB activity but did not influence NOB. Abeliovich and Vonshak (1993) observed complete nitrification inhibition during 4 days of exponentially growing *Nitrosomonas europeana* after 1 hour light exposure, while ammonia presence provided some protection. Alleman *et al.* (1987) observed that light with a wavelength in the range of 410 – 415 nm is responsible for *Nitrosomonas* inhibition, during a period without respiration and nutrient absence. The basis for light sensitivity is assumed to be damage to the many cytochromes of AOB and NOB, involved in the nitrification energy transduction pathways (Ward 2011). No records were found on a longer period of light irradiation and potential adaptation to light inhibiting conditions. Since in this study, no light dark-cycle was used to enable recovery from light inhibition and additionally, the selected light source to stimulated microalgal growth was rich in the inhibitory wavelengths, conditions were unfavourable for nitrifiers.

Theoretically, nitrifying bacteria require 4.57 g oxygen to convert 1 g NH_4^+-N to 0.95 g NO_3^--N and 0.05 g biomass-N, while heterotrophic bacteria consume 0.69 g oxygen to oxidize 1 g of organic carbon to CO_2 (SRT: 6.67 days; 25°C). At day 134, the moment of optimal nitrification, the oxygen consumption and thus production rate was 160 mg O_2 $gVSS^{-1}$ d^{-1}, calculated based on the stoichiometry of nitrogen and organic carbon oxidation. This value is

276 comparable to the photo-oxygenation rates calculated based on the results in other studies
277 (Table 1). Additionally, in this study, the light supply rate was 1.04 mol photons L^{-1} d^{-1}.
278 Together with the volumetric oxygen production rate of 429 mg O_2 L^{-1} d^{-1} (recalculate from
279 160 mg O_2 $gVSS^{-1}$ d^{-1}), this results in an oxygen quantum yield of 0.013 mol O_2 mol photons^{-1}
280 . This is lower than the maximal quantum yield of 0.1 mol O_2 mol photons^{-1} (Zijffers *et al.*
281 2010), indicating room for improvement in photosynthetic efficiency. However, the real
282 photon flux density could be slightly lower due to the lack of perfect homogenous light
283 distribution of 300 µmol photons m^{-2} s^{-1} measured.

284 To check if photosynthetic oxygenation was sufficient, DO was monitored during 1 cycle at
285 day 134 (Figure S8). To assess the oxygen consumption rate without algal oxygen production,
286 the lights were turned off during the first 2 hours. When the DO reached values lower than 3
287 mg O_2 L^{-1}, lights were turned on. Initially the DO remained constant while nitrification was
288 still ongoing, indicating a sufficient photo-oxygenation rate due to the simultaneous oxygen
289 production and consumption. When ammonium and nitrite were fully oxidized (measured
290 with ammonium and nitrite test strips), DO increased in a rate equal to the oxygen production
291 rate minus the heterotrophic oxidation rate. The measured oxygen production rate was 4.24
292 mg O_2 L^{-1} h^{-1} taking into account the ongoing organic carbon oxidation. This oxygen
293 production rate is within the range of other microalgal-bacterial systems (Karya *et al.* 2013).
294 However, 95 mg O_2 L^{-1} was consumed for nitrification and 23 mg O_2 L^{-1} was consumed for
295 COD oxidation leading to a total theoretical oxygen consumption rate of 15 mg O_2 L^{-1} h^{-1}. The
296 difference between this rate and the oxygen consumption rate based on the DO profile might
297 be caused due to the direct consumption of oxygen within the floc entity.

298 *The optimal nitrifying PBR*

299 Since each involved type of micro-organism has its own function, nutritional requirement and
300 metabolic rate, the potential nitrification rate can be calculated. Taking into account the

stoichiometry of photosynthesis, nitrification and heterotrophic COD oxidation, ideally without nitrogen losses, 23% of incoming nitrogen should be assimilated by the microalgae, resulting in a sufficient amount of oxygen to oxidize the leftover 77% of the ammonium nitrogen and present COD (Figure 6). Considering algal oxygen production rates in an optimal designed PBR between 128 and 192 mg O_2 L^{-1} h^{-1} (Javanmardian & Palsson 1992), it is theoretical possible to nitrify urine at a nitrogen influent loading rate of 1.14 g N L^{-1} d^{-1} and 0.91 g COD L^{-1} d^{-1} (urine COD/N ratio of 0.8). In cheaper high-rate algal ponds (HRAP), however, optimal oxygen production rates up to 9.55 mg O_2 L^{-1} h^{-1} are reported (Arbib *et al.* 2017), indicating a maximum influent loading rate of 57 mg N L^{-1} d^{-1}. Ammonia desorption was not considered here, however it was observed before that ammonia desorption is low, providing neutral pH control (Delgadillo-Mirquez *et al.* 2016).

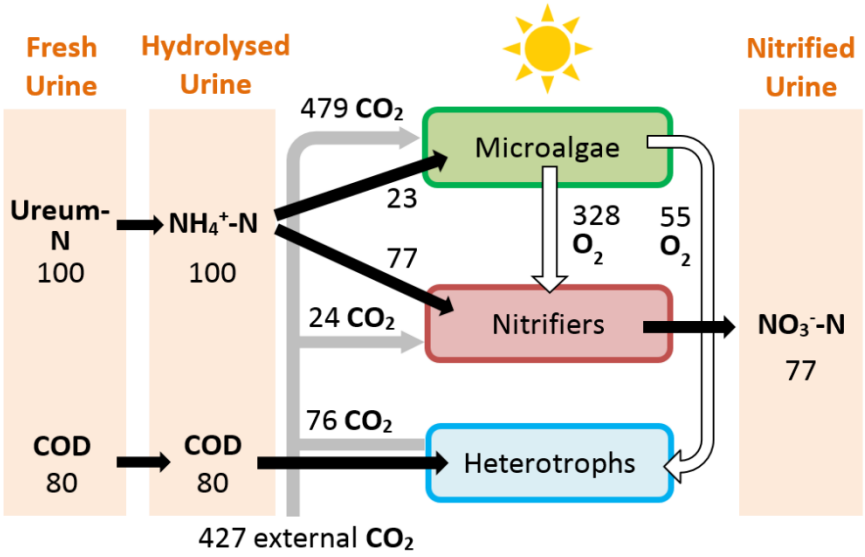

Figure 6. Theoretical behaviour of the ideal consortium of microalgae, nitrifiers and heterotrophs in a nitrifying bioreactor, starting from 100 mass units of ureum nitrogen and 80 mass units of COD (average COD/N mass ratio in urine).

Several operational parameters influence the activity of the consortium organisms. The specific growth rate and activity ratio between microalgae and nitrifying bacteria is influenced by parameters such as available nutrients and light and is related to the substrate affinity constants (K_s) for ammonium nitrogen and inorganic carbon. Due to the higher nitrifier K_s

values for inorganic carbon (21.4 mg C L^{-1}; Guisasola *et al.* (2007)) in comparison to microalgae (0.58 mg C L^{-1}; Shelp and Canvin (1980)), higher CO_2 concentrations favour nitrifiers. The same can be assumed in terms of ammonium concentration due to the lower K_s value for microalgae (0.01 mg N L^{-1}; Hein *et al.* (1995)) compared to AOB (0.42 to 4.47 mg N L^{-1}; Kayee *et al.* (2016)).

Next to high substrate concentrations, an SRT increase favours slow growing nitrifiers and increases nitrification activity. To obtain better settling characteristics, dense floc formation could be stimulated by a low HRT or high volumetric exchange ratio (VER), causing poor-settling biomass to wash out. The microalgae could form the outer layer of the granule while the nitrifying bacteria are protected from light inhibition in the inner layers. Nevertheless, granule formation is a complex process which depends on many parameters. Additionally, the anoxic core could facilitate denitrification, resulting in an unwanted nitrogen loss. With an increase in VER from 15% to 50%, by reducing the amount of cycles from 3 to 2 and increasing the influent flow rate to 2 L d^{-1} of 10% dilution of urine, a nitrogen loading rate of 250 mg N L^{-1} d^{-1} could be reached. Attention has to be paid for potential free ammonia (FA) formation when the same nitrogen loading rate is applied with fewer cycles.

Since parameters such as pH, nutrient quantity and quality, stirring and temperature were optimal for most microalgae, higher oxygen production rates may be achieved by increasing the illuminated volume. Light attenuates exponentially as it penetrates into the culture medium estimated by Lambert-Beer's law (Lee 1999). Ogbonna and Tanaka (2000) observed light penetration of only 2 cm in a photo-bioreactor containing a biomass concentration of 1 g L^{-1} with a light absorption coefficient of 200 m^2 s^{-1} and an illumination intensity of 500 µmol PAR m^{-2} s^{-1}. In this study the photon flux density was 300 µmol PAR m^{-2} s^{-1} and biomass density fluctuated around 2 g VSS L^{-1}, indicating a light penetration depth less than 1 cm or an illuminated volume of less than 30 %.

345 *Microscopy on PBR biomass*

346 Microscopic observation after 180 days of reactor operation revealed that microalgal-bacterial
347 flocs were formed with a size of 50 - 100 µm (Figure 7). *Scenedesmus* sp. was the dominant
348 green microalga present, but also *Chlorella* sp. and the cyanobacteria *Synechocystis* sp. and
349 *Leptolyngbya* sp. were detected. Between the large microalgal cells, the bacteria were present
350 in low numbers. The electrical conductivity in the PBR was fluctuating around 8.5 mS cm^{-1}
351 according with 100 mM NaCl. Among the inoculated microalgae, only *Nannochloropsis* sp.
352 was a distinct salt water species, although all fresh water species were initially cultivated in a
353 salt water medium (ESAW) and depending on species, microalgae can be halotolerant and
354 show adaptation (Hart *et al.* 1991). *Chlorella* sp. presents optimal growth at a salinity level of
355 100 mM (Abdel-Rahman *et al.* 2005), indicating feasible conditions in the PBR. In contrast,
356 for *Scenedesmus obliquus* optimal growth was observed in BBM medium supplemented with
357 25 mM NaCl (Salama *et al.* 2013). This shift towards *Scenedesmus* sp. in a concentrated
358 wastewater solution was observed before by Koreiviene *et al.* (2014), suggesting the larger
359 surface area-to-volume ratio enabled quicker nutrient uptake. Karya *et al.* (2013) inoculated
360 with *Scenedesmus quadricauda* and selection took place towards cyanobacteria, however,
361 reactor salinity was not mentioned.

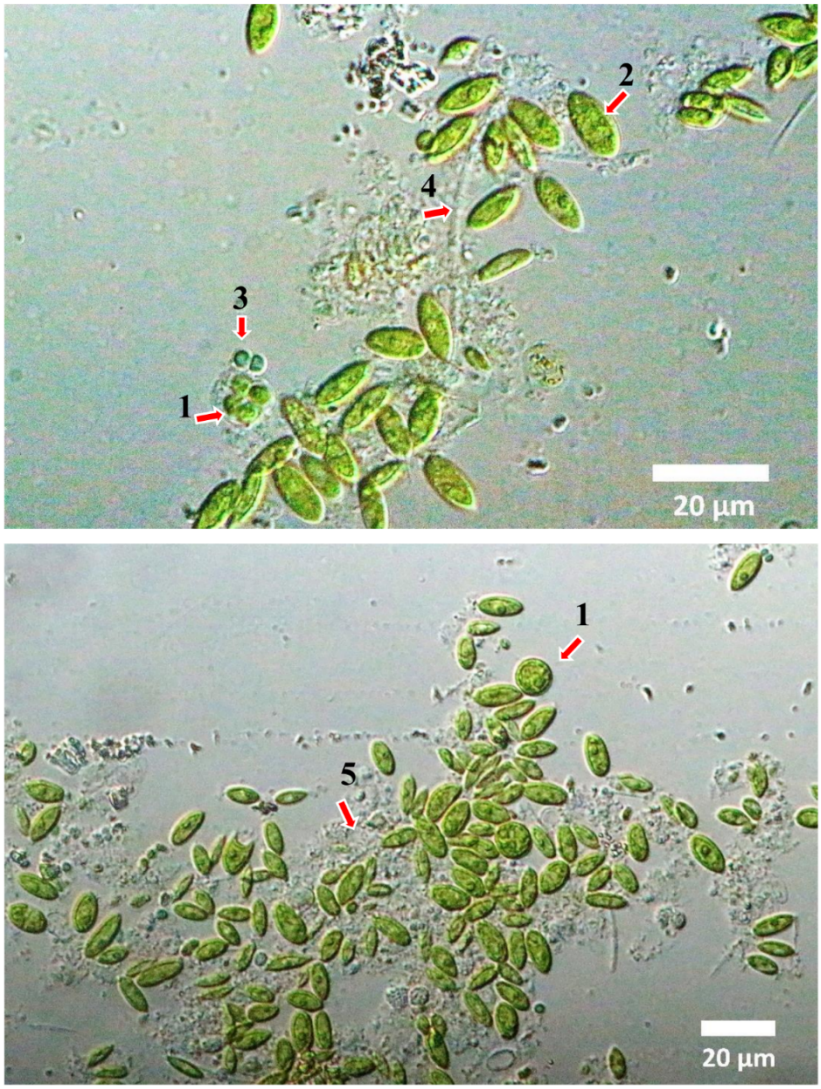

Figure 7. Microscopy on the PBR biomass after 180 days of operation. (1) Chlorella sp.; (2) Scenedesmus sp.; (3) Synechocystis sp.; (4) Leptolyngbya sp.; (5) Bacteria.

Potential applications for photosynthetic oxygenation

Since the energy gain of photosynthetic oxygenation would completely disappear in a photo-bioreactor with synthetic light supply, high-rate algal ponds and photo-bioreactors in natural sunlight are more suitable. Although electricity costs and associated carbon footprint are reduced and electricity independence allows application in developing countries, the volumetric nitrification rate of 67 mg N L^{-1} d^{-1} achieved in this study is low compared to the urine nitrification rate of 450 mg N L^{-1} d^{-1} achieved with conventional aeration in a membrane bioreactor (Coppens *et al.* 2016). Due to this lower nitrification rate and outdoor day-night light regime, the required surface area and reactor volume are higher compared to systems

relying on conventional aeration. Outdoor experiments on a larger scale should be performed to get a better sight on the true energy gain of photosynthetic oxygenation.

Conclusion

It was experimentally demonstrated that biological oxidation of all nitrogen present in urine to nitrate is a promising pre-treatment stabilization step to substitute expensive conventional aeration, before further nutrient recovery. A consortium of microalgae and nitrifying bacteria was successfully developed in which the **photosynthetic oxygenation** rate was sufficiently high to nitrify urine at a volumetric nitrification rate of 67 mg N L^{-1} d^{-1}. Additionally, a maximum biomass specific photo-oxygenation rate of 160 mg O_2 $gVSS^{-1}$ d^{-1} was achieved and microscopic observations revealed that *Scenedesmus* sp. was the dominant microalga after 180 days of reactor operation. Finally, outdoor experiments on a larger scale should be performed to estimate the true energy gain of photosynthetic oxygenation.

Acknowledgement

The authors would like to thank Dr. Claudio Sili from the ISE-CNR, Firenze for determination of the microalgae and Dr. Marc Spiller and Dr. ir. Erik Van Eynde for the critical discussions. This study was also supported by the European Space Agency (ESA) and the Belgian Science Policy (BELSPO) in the framework of the MELiSSA project.

References

Abdel-Rahman M. H. M., ALi R. M. and Said H. A. 2005 Alleviation of NaCl-induced Effects on Chlorella vulgaris and Chlorococcum humicola by Riboflavin Application *International Journal of Agriculture & Biology*, **7**(1), 58-62.

Abeliovich A. and Vonshak A. 1993 Factors Inhibiting Nitrification of Ammonia in Deep Waste-Water Reservoirs. *Water Research*, **27**(10), 1585-90.

Adamsson M. 2000 Potential use of human urine by greenhouse culturing of microalgae (Scenedesmus acuminatus), zooplankton (Daphnia magna) and tomatoes (Lycopersicon). *Ecological Engineering*, **16**(2), 243-54.

Alleman J. E., Keramida V. and Panteakiser L. 1987 Light-Induced Nitrosomonas Inhibition. *Water Research*, **21**(4), 499-501.

Arbib Z., Crespo I. D., Corona E. L. and Rogalla F. 2017 Understanding the biological activity of high rate algae ponds through the calculation of oxygen balances. *Applied Microbiology and Biotechnology*, **101**(12), 5189-98.

Basakcilardan-Kabakci S., Ipekoglu A. N. and Talini I. 2007 Recovery of ammonia from human urine by stripping and absorption. *Environmental Engineering Science*, **24**(5), 615-24.

Brooks T. and Keevil C. W. 1997 A simple artificial urine for the growth of urinary pathogens. *Letters in Applied Microbiology*, **24**(3), 203-6.

Coppens J., Lindeboom R., Muys M., Coessens W., Alloul A., Meerbergen K., Lievens B., Clauwaert P., Boon N. and Vlaeminck S. E. 2016 Nitrification and microalgae cultivation for two-stage biological nutrient valorization from source separated urine. *Bioresource Technology*, **211**, 41-50.

de Godos I., Blanco S., Garcia-Encina P. A., Becares E. and Munoz R. 2009 Long-term operation of high rate algal ponds for the bioremediation of piggery wastewaters at high loading rates. *Bioresource Technology*, **100**(19), 4332-9.

Delgadillo-Mirquez L., Lopes F., Taidi B. and Pareau D. 2016 Nitrogen and phosphate removal from wastewater with a mixed microalgae and bacteria culture. *Biotechnology Reports*, **11**(Supplement C), 18-26.

Feng D. L., Wu Z. C. and Xu S. H. 2008 Nitrification of human urine for its stabilization and nutrient recycling. *Bioresource Technology*, **99**(14), 6299-304.

Greenberg A. E., Clesceri L. S. and Eaton A. D. 1992 Standard methods for the examination of waste and wastewater. In, American Public Health Society, Washington.

Guerrero M. A. and Jones R. D. 1996 Photoinhibition of marine nitrifying bacteria .2. Dark recovery after monochromatic or polychromatic irradiation. *Marine Ecology Progress Series*, **141**(1-3), 193-8.

Guisasola A., Petzet S., Baeza J. A., Carrera J. and Lafuente J. 2007 Inorganic carbon limitations on nitrification: Experimental assessment and modelling. *Water Research*, **41**(2), 277-86.

Gutzeit G., Lorch D., Weber A., Engels M. and Neis U. 2005 Bioflocculent algal-bacterial biomass improves low-cost wastewater treatment. *Water Science and Technology*, **52**(12), 9-18.

Harrison P. J., Waters R. E. and Taylor F. J. R. 1980 A Broad-Spectrum Artificial Seawater Medium for Coastal and Open Ocean Phytoplankton. *Journal of Phycology*, **16**(1), 28-35.

Hart B. T., Bailey P., Edwards R., Hortle K., James K., Mcmahon A., Meredith C. and Swadling K. 1991 A Review of the Salt Sensitivity of the Australian Fresh-Water Biota. *Hydrobiologia*, **210**(1-2), 105-44.

Hein M., Pedersen M. F. and Sandjensen K. 1995 Size-Dependent Nitrogen Uptake in Micro- and Macroalgae. *Marine Ecology Progress Series*, **118**(1-3), 247-53.

Javanmardian M. and Palsson B. O. 1992 Design and Operation of an Algal Photobioreactor System. *Life Sciences and Space Research Xxiv (4) : Natural and Artificial Ecosystems*, **12**, 231-5.

Karya N. G. A. I., van der Steen N. P. and Lens P. N. L. 2013 Photo-oxygenation to support nitrification in an algal-bacterial consortium treating artificial wastewater. *Bioresource Technology*, **134**, 244-50.

Kayee P., Rongsayamanont C., Kunapongkiti P. and Limpiyakorn T. 2016 Ammonia half-saturation constants of sludge with different community compositions of ammonia-oxidizing bacteria. *Environmental Engineering Research*, **21**(2), 140-4.

Koreiviene J., Valciukas R., Karosiene J. and Baltrenas P. 2014 Testing of Chlorella/Scenedesmus Microalgae Consortia for Remediation of Wastewater, Co2

Mitigation and Algae Biomass Feasibility for Lipid Production. *Journal of Environmental Engineering and Landscape Management*, **22**(2), 105-14.
Kuai L. P. and Verstraete W. 1998 Ammonium removal by the oxygen-limited autotrophic nitrification-denitrification system. *Applied and Environmental Microbiology*, **64**(11), 4500-6.
Kujawa-Roeleveld K. and Zeeman G. 2006 Anaerobic treatment in decentralised and source-separation-based sanitation concepts. *Reviews in Environmental Science and Biotechnology*, **5**(1), 115-39.
Lee C.-G. 1999 Calculation of light penetration depth in photobioreactors. *Biotechnol. Bioprocess Eng.*, **4**, 78-81.
Maurer M., Pronk W. and Larsen T. A. 2006 Treatment processes for source-separated urine. *Water Research*, **40**(17), 3151-66.
Metcalf & Eddy I. (2002). *Wastewater Engineering: Treatment and Reuse*. McGraw-Hill, Boston
Ogbonna J. C. and Tanaka H. 2000 Light requirement and photosynthetic cell cultivation - Development of processes for efficient light utilization in photobioreactors. *Journal of Applied Phycology*, **12**(3-5), 207-18.
Praveen P. and Loh K. C. 2015 Photosynthetic aeration in biological wastewater treatment using immobilized microalgae-bacteria symbiosis. *Applied Microbiology and Biotechnology*, **99**(23), 10345-54.
Salama E. S., Kim H. C., Abou-Shanab R. A. I., Ji M. K., Oh Y. K., Kim S. H. and Jeon B. H. 2013 Biomass, lipid content, and fatty acid composition of freshwater Chlamydomonas mexicana and Scenedesmus obliquus grown under salt stress. *Bioprocess and Biosystems Engineering*, **36**(6), 827-33.
Shelp B. J. and Canvin D. T. 1980 Utilization of Exogenous Inorganic Carbon Species in Photosynthesis by Chlorella-Pyrenoidosa. *Plant Physiology*, **65**(5), 774-9.
Tsioptsias C., Lionta G. and Samaras P. 2017 Microalgae-activated sludge treatment of molasses wastewater in sequencing batch photo-bioreactor. *Environmental Technology*, **38**(9), 1120-6.
Tuantet K., Janssen M., Temmink H., Zeeman G., Wijffels R. H. and Buisman C. J. N. 2013 Microalgae growth on concentrated human urine. *Journal of Applied Phycology*.
Udert K. M., Larsen T. A., Biebow M. and Gujer W. 2003 Urea hydrolysis and precipitation dynamics in a urine-collecting system. *Water Research*, **37**(11), 2571-82.
Udert K. M., Larsen T. A. and Gujer W. 2006 Fate of major compounds in source-separated urine. *Water Science and Technology*, **54**(11-12), 413-20.
van der Steen P., Rahsilawati K., Rada-Ariza A. M., Lopez-Vazquez C. M. and Lens P. N. L. 2015 A new photo-activated sludge system for nitrification by an algal-bacterial consortium in a photo-bioreactor with biomass recycle. *Water Science and Technology*, **72**(3), 443-50.
Vergara C., Munoz R., Campos J. L., Seeger M. and Jeison D. 2016 Influence of light intensity on bacterial nitrifying activity in algal-bacterial photobioreactors and its implications for microalgae-based wastewater treatment. *International Biodeterioration & Biodegradation*, **114**, 116-21.
Verstraete W., Clauwaert P. and Vlaeminck S. E. 2016 Used water and nutrients: Recovery perspectives in a 'panta rhei' context. *Bioresource Technology*, **215**, 199-208.
Ward B. B. 2011 Measurement and Distribution of Nitrification Rates in the Oceans. *Methods in Enzymology: Research on Nitrification and Related Processes, Vol 486, Part A*, **486**, 307-23.
Yang C. L., Liu H., Li M., Yu C. Y. and Yu G. 2008 Treating urine by Spirulina platensis. *Acta Astronautica*, **63**(7-10), 1049-54.

Zijffers J. W. F., Schippers K. J., Zheng K., Janssen M., Tramper J. and Wijffels R. H. 2010 Maximum Photosynthetic Yield of Green Microalgae in Photobioreactors. *Marine Biotechnology*, **12**(6), 708-18.

Supplementary material

Photosynthetic oxygenation for urine nitrification

Maarten Muys[1], Joeri Coppens[2], Nico Boon[2] , Siegfried E. Vlaeminck[1, 2, *]

[1] Research Group of Sustainable Energy, Air and Water Technology, Department of Bioscience Engineering, University of Antwerp, Groenenborgerlaan 171, 2020 Antwerpen, Belgium.

[2] Center for Microbial Ecology and Technology (CMET), Ghent University, Coupure Links 653, 9000 Gent, Belgium.

[*] Corresponding author: Siegfried.Vlaeminck@UAntwerpen.be

Table S1. Operational events during PBR operation.

Event	Time (d)	Operation	Average HRT (d)
A	15	Re-inoculation with ABIL activated sludge	13.3
B	25	Co-aeration with compressed air ON	13.3
C	34	Increase in N-loading rate from 50 mg N L^{-1} d^{-1} to 75 mg N L^{-1} d^{-1}	6.7
D	119	Co-aeration with compressed air OFF	6.7
E	125	Increase in N-loading rate from 75 mg N L^{-1} d^{-1} to 90 mg N L^{-1} d^{-1}	6.7
F	134	Increase in N-loading rate from 90 mg N L^{-1} d^{-1} to 100 mg N L^{-1} d^{-1}	6.7

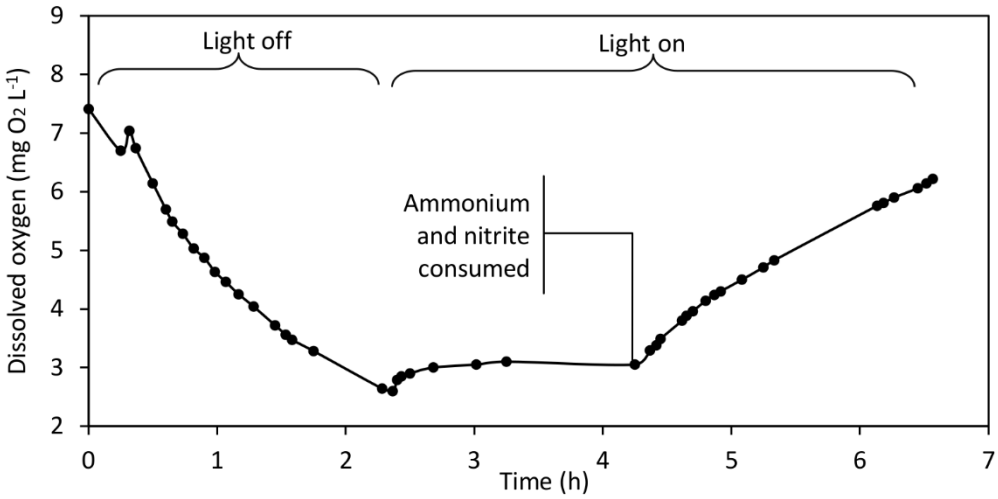

Figure S8. Dissolved oxygen profile in the PBR during one cycle at day 134, in which an introduced dark phase visualises the oxygen consumption rate.

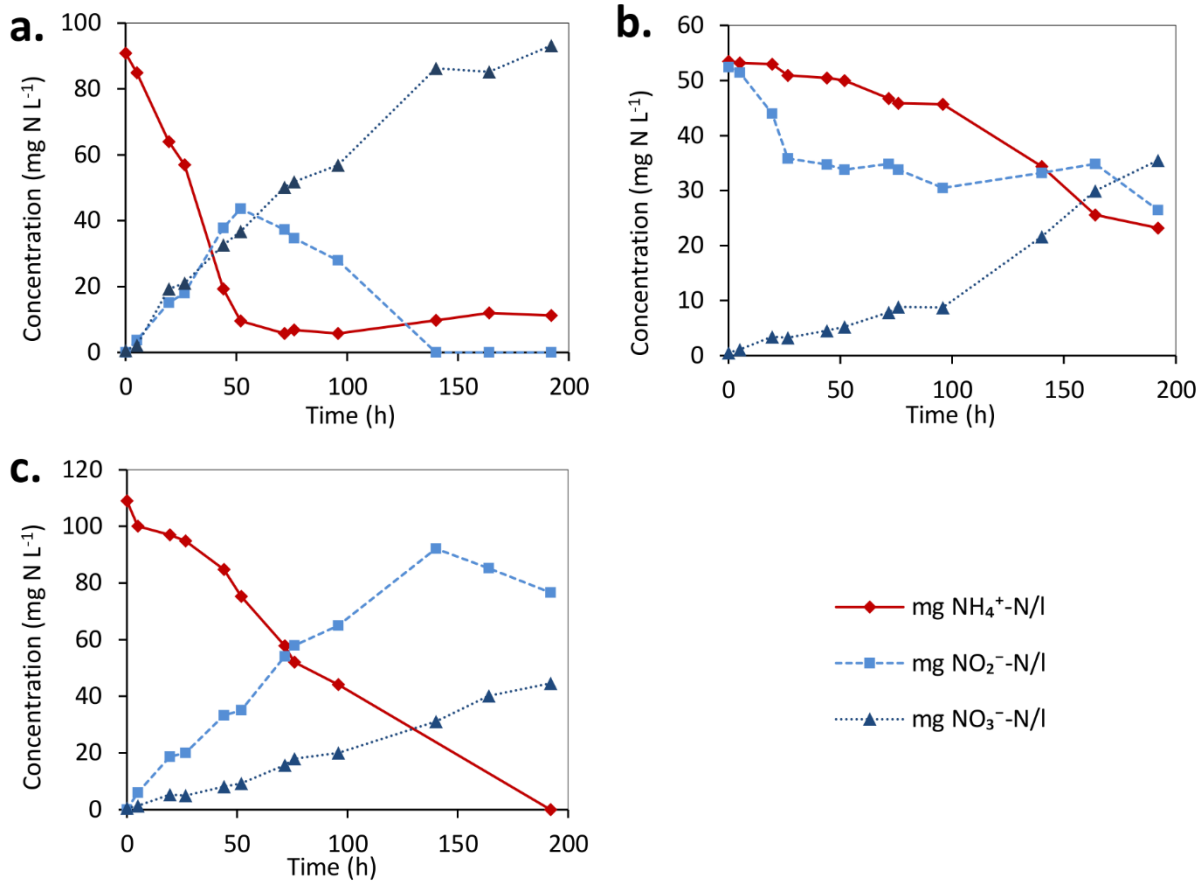

Figure S9. Day 19 nitrification activities in batch for both AOB and NOB in which (a) new nitrifying inoculum was exposed to fresh medium and (b) PBR biomass to fresh medium and (c) PBR effluent.

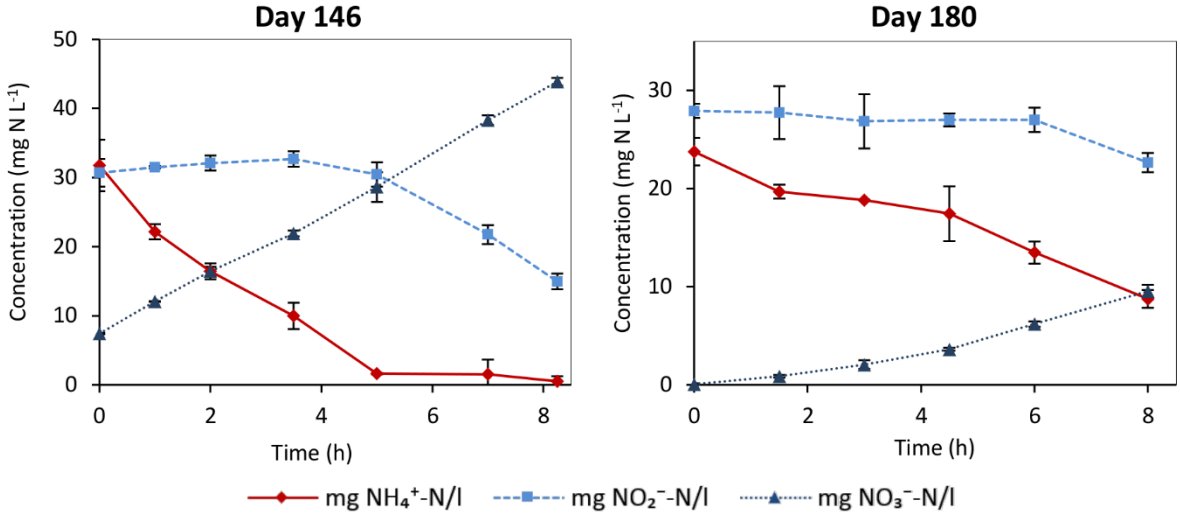

Figure S10. PBR biomass nitrification activities for both AOB and NOB in batch after 146 days and after 180 days.